Optimization of n-PERT Solar Cell under Atacama Desert Solar Spectrum

Pablo Ferrada Martínez

Benjamín Ivorra, Miriam Ruiz Ferrández, Emilio Ruiz Reina

June 9, 2022

Master's Degree in Numerical Simulation in Science and Engineering with COMSOL Multiphysics

Introduction: Solar resource in the world

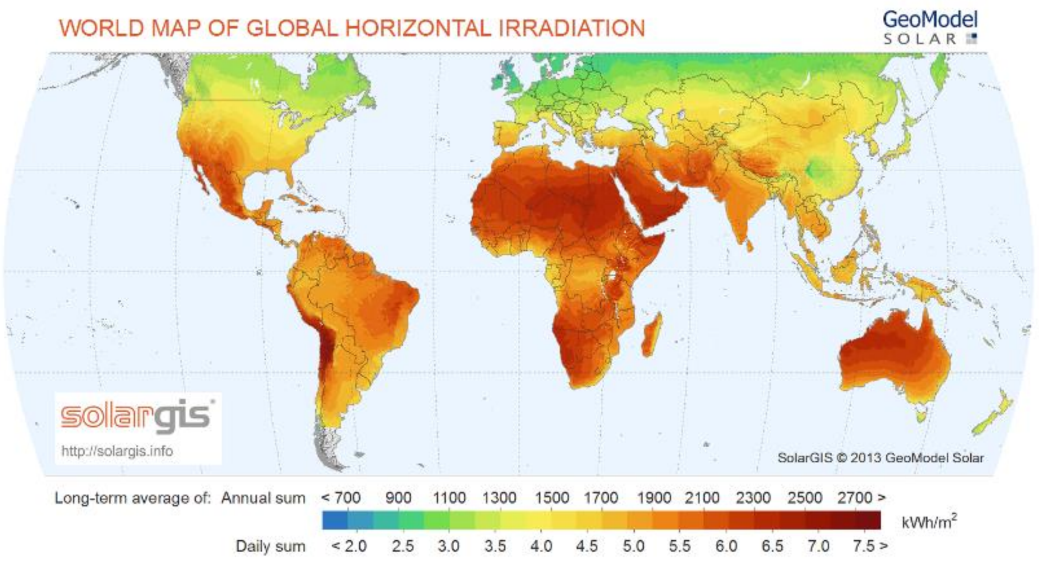

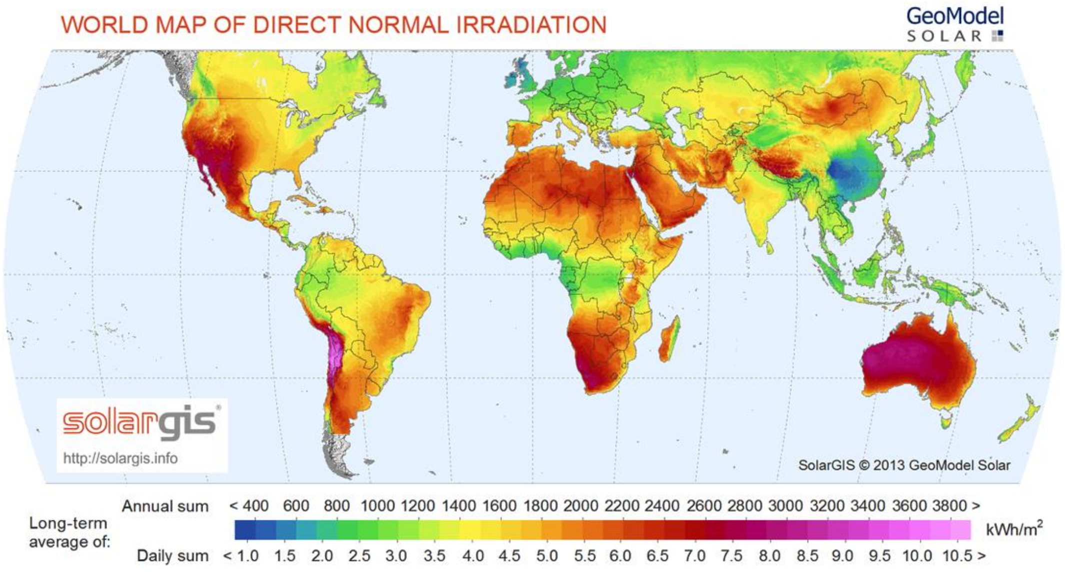

- 5.6% of Reference Spectrum (AM1.5G) is UVA + UVB for the Tilted Global Irradiance (GTI).
- Atacama Desert receives the highest irradiation in the world, with 7.7% of its energy in the UV range.

A. Marzo, P. Ferrada. Standard or local solar spectrum? Implications for solar technologies studies in the Atacama desert. Renewable Energy 127 (2018), 871-882

Introduction: Solar Spectrum in the Atacama Desert

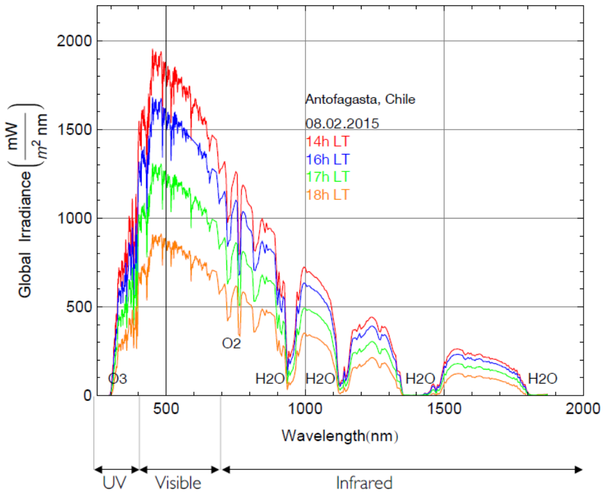

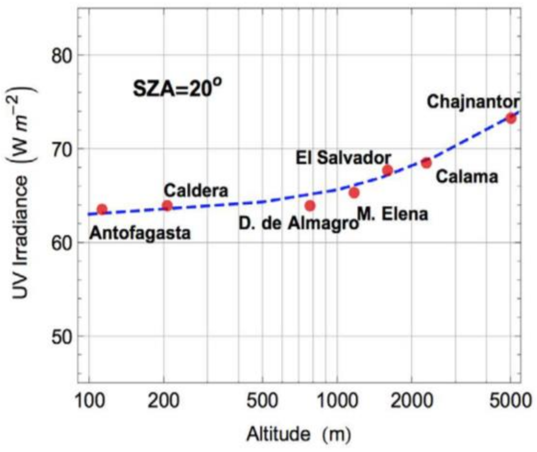

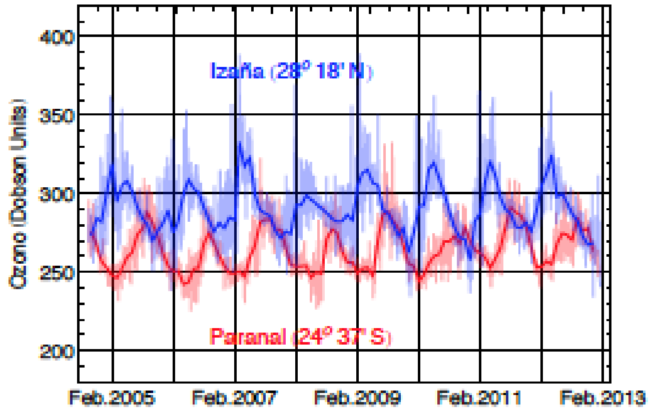

Irradiance = *f* (atmospheric composition)

Total **O**zone **C**olumn (TOC)→ UV-B
Aerosol **O**ptical **D**epth (AOD)
Precipitable **W**ater (PW)
Optical **P**ath **L**ength in atmosphere (altitude)

Interhemispheric differences in TOC

→ Annual dose of UV-B is **35-65% higher in Atacama** than in the south of EU.

→ Degradation

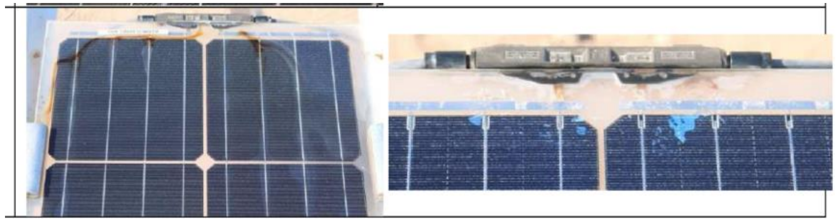

Solar Energy Materials & Solar Cells 236 (2022) 111508

R. Cordero et al. *The Solar Spectrum of Atacama Desert*. Scientific Reports 6, Article number: 22457 (2016).
R. Cordero et al. "*Ultraviolet radiation in the Atacama Desert*". Antonie Van Leeuwenhoek. 2018;111(8):1301-1313.

Problem description

- There are differences with respect to reference spectrum: intensity and UV content.
  - → Desert Label for Atacama Desert
- Solar cell is designed for high efficiency under standard testing conditions (STC).
  - → AM1.5G spectrum, 1000 W/m^2 and 25 °C.
- The PV device exhibits losses when operating at non-standard conditions (no optimum).

F. Lelievre,...,A. Marzo, P. Ferrada et al. *Desert label development for improved reliability and durability of PV modules in harsh desert conditions*. Solar Energy Materials & Solar Cells 236 (2022) 111508.

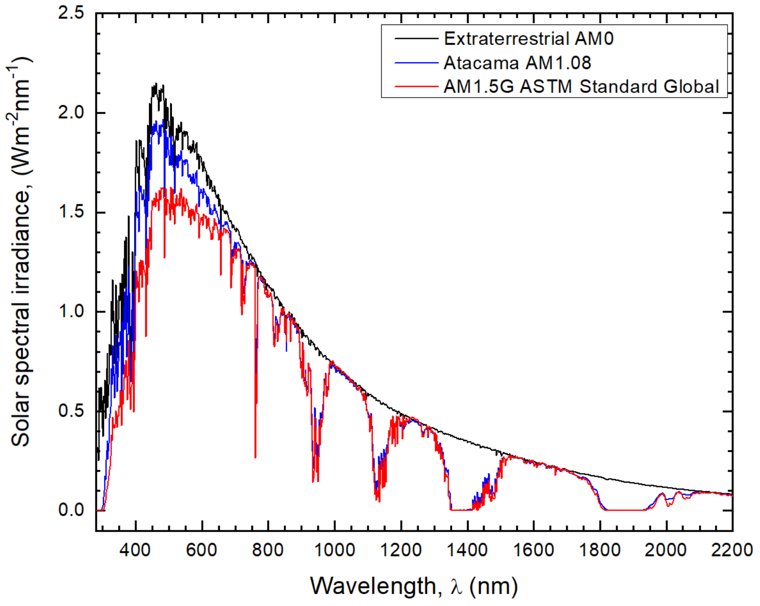

A Marzo, P Ferrada "*Standard or Local Solar Spectrum? Implications for Solar Technologies Studies in Atacama Desert*". Ren. En. 127 (2018), 871.

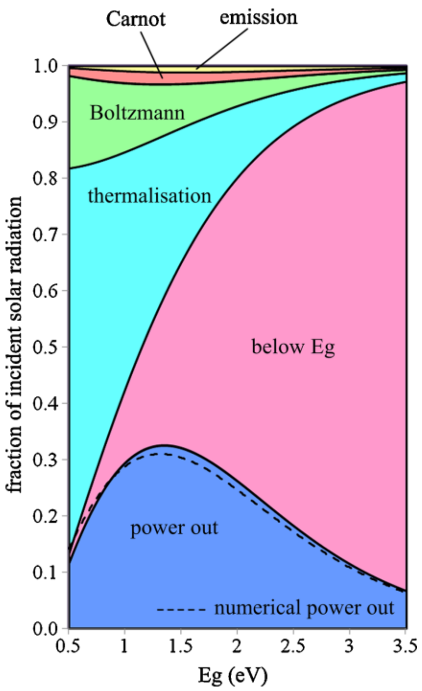

L. C. Hirst, N. J. Ekins-Daukes. *Fundamental losses in solar cells*. Prog. Photovolt: Res. Appl. 2011; 19:286–293.

Objectives

- To determine optimal parameters of a n-PERT cell when operating under Atacama Desert spectral conditions.
- To compute the characteristic curve of an optimized n-PERT cell for a whole day in Atacama Desert.

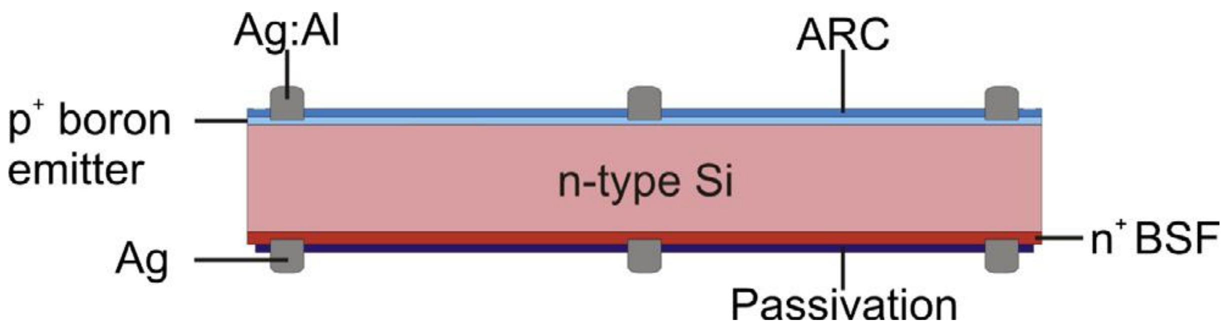

n-PERT

n-type **p**assivated **e**mitter and **r**ear **t**otally diffused

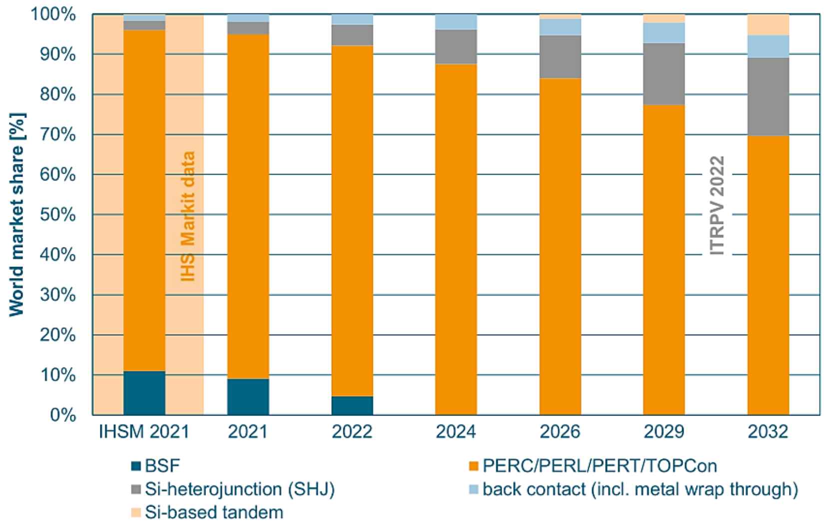

P. Ferrada, A. Marzo et al. “*Potential for photogenerated current for Si based PV modules in the Atacama Desert*”, Solar Energy 144 (2017), 580-593.

International Technology Roadmap of Photovoltaics (ITRPV) 2022.

Materials & methods: Stages

1. Validation

   1.1 Fabricate a standard n-PERT solar cell.

   1.2 Model/simulate the n-PERT under AM1.5G.

   -Mesh Independence study

   1.3 Explain differences and improve the model.

2. Optimization

   2.1 Define *obj func*, *control par*, *const* and *output var*.

   2.2 Configure COMSOL + MATLAB for optimization.

3. Prediction

   3.1 Use fixed and optimized inputs in the model.

   3.2 Calculate the JV curve for a whole day in Atacama D.

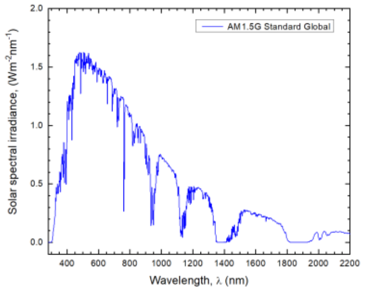

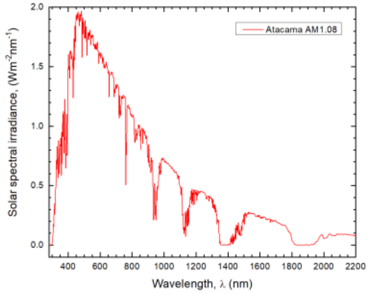

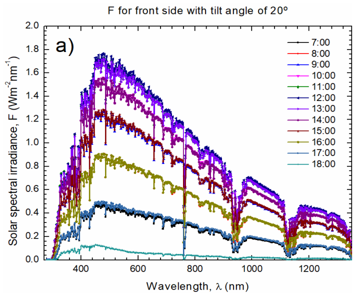

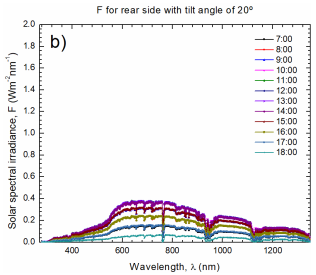

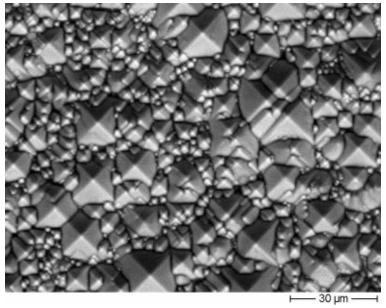

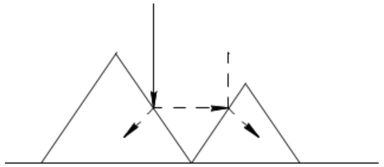

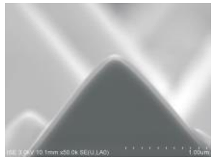

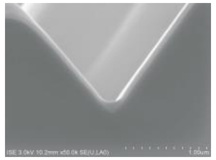

Higher Surface area:

→ Higher absorption and less reflection ($J_{sc,meas}$=1.17 $J_{sc,calc}$)

→ Higher recombination rate (1.7 times more)

A. Fell et al. ***Input Parameters for the Simulation of Silicon Solar Cells in 2014.*** **IEEE Journal of PV 5 (2015), 1250–1263**

UNIVERSIDAD DE MÁLAGA | uma.es

Materials & methods: Model and optimization

- Model: COMSOL
  - Semiconductor Module
  - Geometry: 1D object
  - Material: c-Si
  - Stationary study
    Parametric Sweep over voltage
  - Direct Solver: MUltifrontal Massively Parallel Solver (MUMPS)
  - 5 dependent variables.
    Electron concentration, Ne
    Hole concentration, Ph
    Boundary electron concentration, n_bnd
    Boundary hole concentration, p_bnd
    Electric potential, V

- Optimization in MATLAB
  - Function nPERTopt(x) from COMSOL saved as *m
  - Genetic Algorithm (GA)
  - Script containing input parameters for the GA

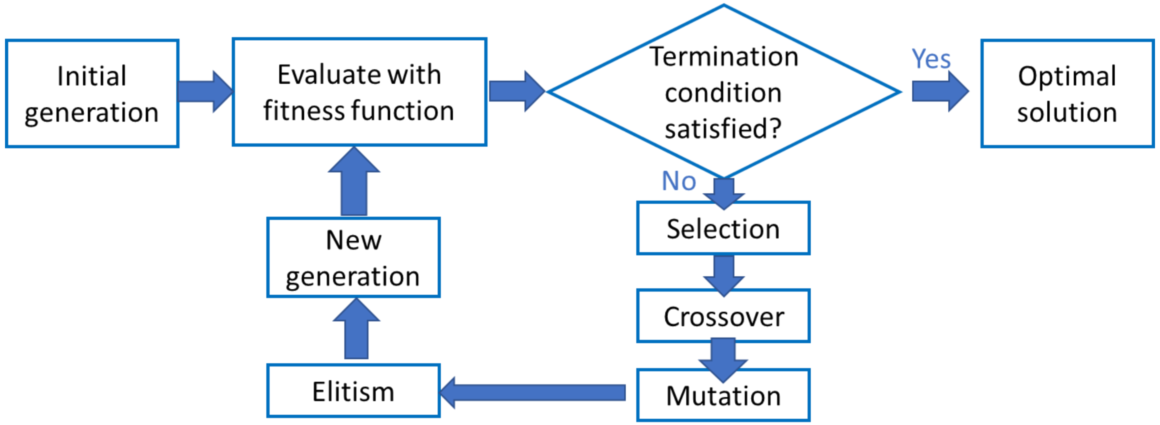

UNIVERSIDAD DE MÁLAGA | uma.es

Theory: Poisson, drift-diffusion, continuity

Poisson equation $\nabla\cdot(-\varepsilon_r\nabla V)=\rho$

Net charge $\rho=q(p-n+N_d^+-N_a^-)$

Electron Conc. $n=N_C F_{1/2}\left(-\frac{E_c-E_{fn}}{k_BT}\right)$ $N_C=2\left(\frac{m_e^*k_BT}{2\pi\hbar^2}\right)^{3/2}$

Hole Conc. $p=N_V F_{1/2}\left(-\frac{E_{fp}-E_v}{k_BT}\right)$ $N_V=2\left(\frac{m_h^*k_BT}{2\pi\hbar^2}\right)^{3/2}$

Fermi Integral $F_{1/2}(\eta_c)=\int_0^\infty\frac{{\eta_c}^{1/2}}{1+e^{x-\eta_c}}dx$

Relative permittivity of silicon	ε_r
Charge density	ρ [C/cm^3]
Electron, hole concentration	n, p [cm^{-3}]
Ionized donor, acceptor impurity	N_d^+, N_A^- [cm^{-3}]
Eff. Density of states in Cond. Band	N_C [cm^{-3}]
Eff. Density of states in Val. Band	N_V [cm^{-3}]
Quasi Fermi levels	E_{fn}, E_{fp} [eV]
Equilibrium Fermi Level	E_{f0}[eV]
Temperature	T [K]

Doping $N=N_0\exp((-d/l)^2)$

Decay length $l=d_j/\sqrt{ln([N_0/N_b])}$

P. Altermatt. Models for numerical device simulations of crystalline silicon solar cells—a review. J Comput Electron (2011) 10:314–330.

Theory: Poisson, drift-diffusion, continuity

Transport for electrons (e) $\boldsymbol{J_n} = qn\mu_n(N_d^+, T)\boldsymbol{E} + \mu_n k_B T g\left(\frac{n}{N_C}\right)\nabla n + qnD_{n,th}\nabla \ln(T)$

Transport for holes (h) $\boldsymbol{J_p} = qp\mu_p(N_a^-, T)\boldsymbol{E} - \mu_p k_B T g\left(\frac{p}{N_V}\right)\nabla p - qpD_{p,th}\nabla \ln(T)$

Continuity for e and h $\frac{\partial n}{\partial t} = \frac{1}{q}(\nabla \cdot \boldsymbol{J_n}) - U_n$ $\frac{\partial p}{\partial t} = -\frac{1}{q}(\nabla \cdot \boldsymbol{J_p}) - U_p$

Net e, h Recombination $U_n = \sum R_{n,i} - \sum G_{n,i}$ $U_p = \sum R_{p,i} - \sum G_{p,i}$

Generation rate for e and h: $G(z) = \frac{4\pi}{hc}(1 - f_{met}) \int_{\lambda_1}^{\lambda_2} \kappa(\lambda)\, F(\lambda)\, e^{-\frac{4\pi\,\kappa\, z}{\lambda}}[1 - R(\lambda)]d\lambda$

Current density for e, h
J_n, J_p [mA/cm²]

Electron, hole mobility
μ_n, μ_p [cm²/(V s)]

Thermal diffusion coefficient
$D_{n,th}, D_{p,th}$ [cm²/s]

Electric field
$\boldsymbol{E}$ [V/m]

Recombination rate
R_n, R_p [1/(cm³ s)]

Solar spectral irradiance
$F(\lambda)$ [W/(m² nm))]

Extinction coefficient
κ

Spectral reflection
$R(\lambda)$

Results & discussion : Validation

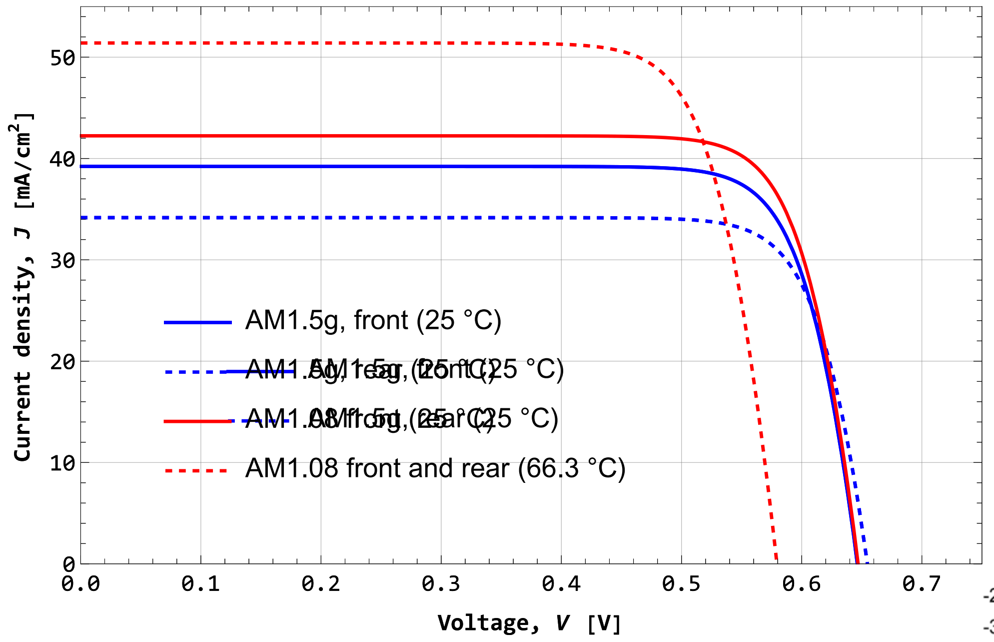

	IV measurement		IV simulation		Relative difference (%)	
Parameter	Front side	Rear side	Front side	Rear side	Front side	Rear side
J_{sc} (mA/cm^2)	39.2 ± 0.03	34.6 ± 0.03	39.2	34.2	0.1	1.3
V_{oc} (mV)	653.1 ± 2	649.7 ± 2	646.4	654.6	1.0	0.8
P_{mpp} (W)	4.9 ± 0.02	4.3 ± 0.09	5.3	4.6	8.3	6.9
FF (%)	78.3 ± 0.2	78.2 ± 0.16	78.7	78.7	0.5	0.6
η (%)	20 ± 0.08	17.6 ± 0.1	20.0	18.0	0.3	<0.1

- Variation in f_{met}
- Reduction in V_{oc} for p⁺-type emitter
  - 45 mV due to front metallization
  - 35 mV due to rear metallization
- $P_{mpp} = P_{mpp,0} - R_{ser}I_{mpp}{}^2$

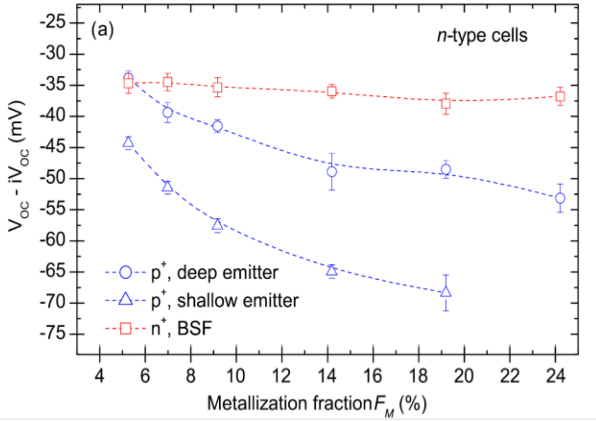

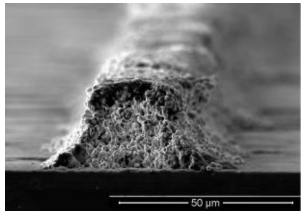

Edler et al. *Metallization-induced recombination losses of bifacial silicon solar cells*. Prog. Photovolt: Res. Appl. 2015; 23:620–627.

Correa. *Electrical conduction in the Ag/si interface of Si solar cells*. 9th International Conference on Low Dimensional Structures and Devices, 2-6 December 2019At: Puerto Varas, Chile.

Results & discussion: Optimization in MATLAB

Inputs of the Genetic Algorithm

	[d_E, d_{cell}, d_{BSF}, N_E, N_B, N_{BSF}]
Maximum values (xmin):	[0.2, 150, 0.2, 1e19, 1e14, 1e19]
Minimum values (xmax):	[1, 200, 1, 1e20, 1e15, 5e20]

Population size (Npop): 70
Generation N° (Ngen): 110
Stop criterium (Nsic): 10
Mutation probability (pmut): 0.1
Refinement (resfin): 0

Function to minimize

```
P=-model.result.numerical('pev1').getReal;
```

Description	Parameter	Initial values	AM1.5g	AM1.08
Emitter thickness	d_E (um)	0.65	0.20	0.20
Cell thickness	d_{cell} (um)	180	150	150
BSF thickness	d_{BSF} (um)	0.45	0.33	0.25
Emitter doping	N_E (cm^{-3})	2.44×10^{19}	9.89×10^{19}	9.36×10^{19}
Base doping	N_B (cm^{-3})	8.44×10^{14}	9.83×10^{14}	9.84×10^{14}
BSF doping	N_{BSF} (cm^{-3})	6.16×10^{19}	3.87×10^{20}	4.12×10^{20}

Results & discussion : Cell response, optimized to Atacama Spectrum

- JV of optimized solar cell to AM1.5g and AM1.08
- Table with the JV parameters
  - Optimized case
  - Non-optimized cell

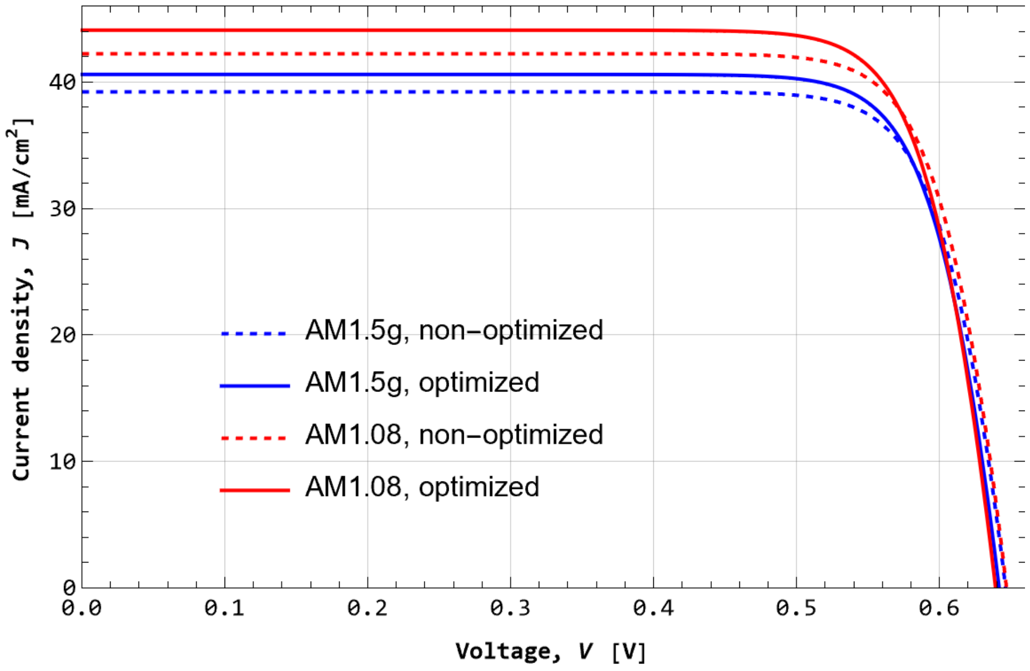

	Optimized case				
	J_{sc} (mA/cm^2)	V_{oc} (mV)	P_{mpp} (W)	FF (%)	Eta (%)
Standard AM1.5g	40.6	641.7	5.5	82.3	21.5
Atacama AM1.08	44.1	639.2	5.9	83.0	23.4

	Non-optimized case				
	J_{sc} (mA/cm^2)	V_{oc} (mV)	P_{mpp} (W)	FF (%)	Eta (%)
Standard AM1.5g	39.2	646.4	5.3	78.7	20.0
Atacama AM1.08	42.2	647.0	5.7	78.9	21.6

	Comparison though the relative difference				
	J_{sc}	V_{oc}	P_{mpp}	FF	Eta
Standard AM1.5g	3.6%	-0.7%	4.3%	4.6%	7.6%
Atacama AM1.08	4.3%	-1.2%	4.7%	5.2%	8.5%

$$100\,(X_{opt} - X_{non\text{-}opt}) / X_{non\text{-}opt}$$

Results & discussion : Java

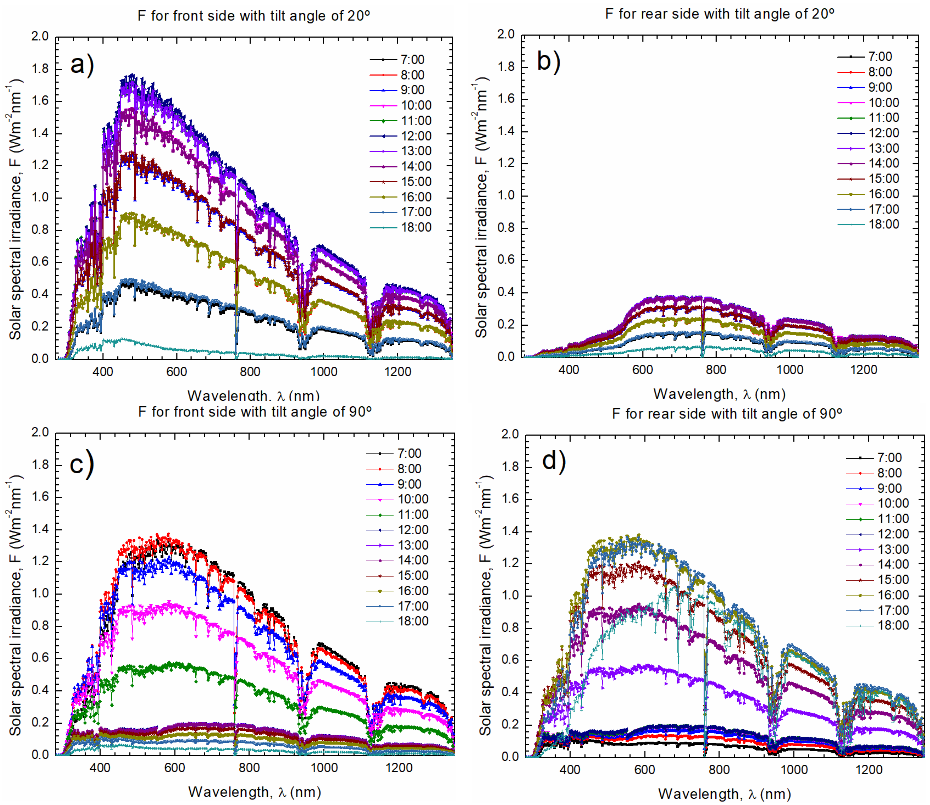

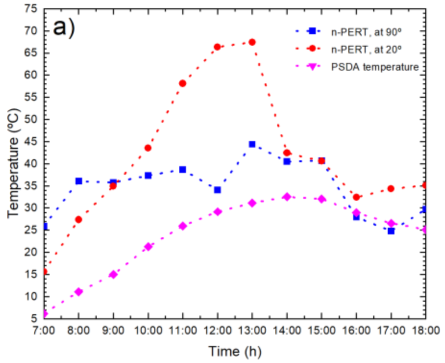

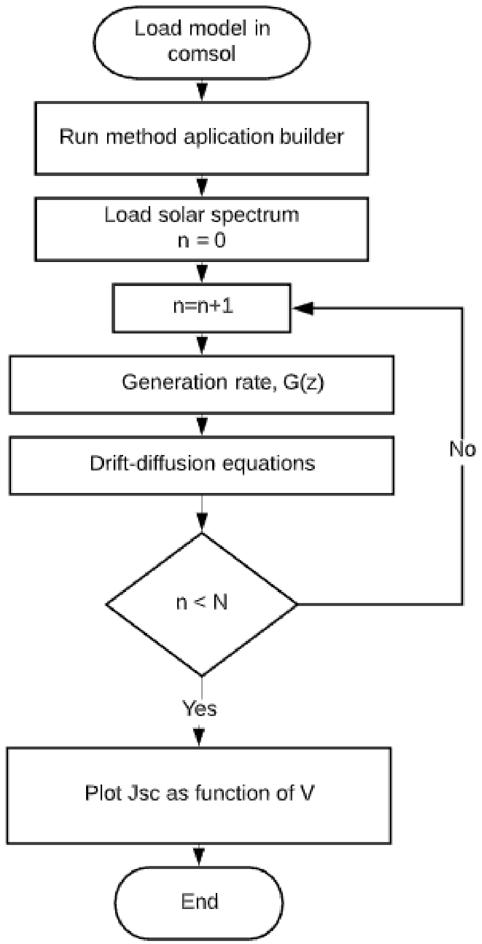

$$G(z) = \frac{4\pi}{hc}\left(1 - f_{m,f}\right)\int_{\lambda_1}^{\lambda_2} \kappa(\lambda)\, F_f(\lambda)\, e^{-\frac{4\pi\,\kappa\, z}{\lambda}}\left[1 - R_f(\lambda)\right] d\lambda + \frac{4\pi}{hc}\left(1 - f_{m,r}\right)\int_{\lambda_1}^{\lambda_2} \kappa(\lambda)\, F_r(\lambda)\, e^{-\frac{4\pi\,\kappa\, z}{\lambda}}\left[1 - R_r(\lambda)\right] d\lambda$$

A. Fell et al. *Simplified Device Simulation of Silicon Solar Cells Using a Lumped Parameter Optical Model*. Journal of Photovoltaics 6:3 (2016), 611-616.

M. M. Chowdhury. *Approximation of Carrier Generation Rate in Common Solar Cells and Studies for Optimization of n⁺p Silicon Solar Cell for AM1.5G and AM1.5D*. 2012 7th Int. Conf. on Electrical and Computer Engineering 20-22 December 2012, Dhaka, Bangladesh.

Results & discussion : Response for different spectra along the day

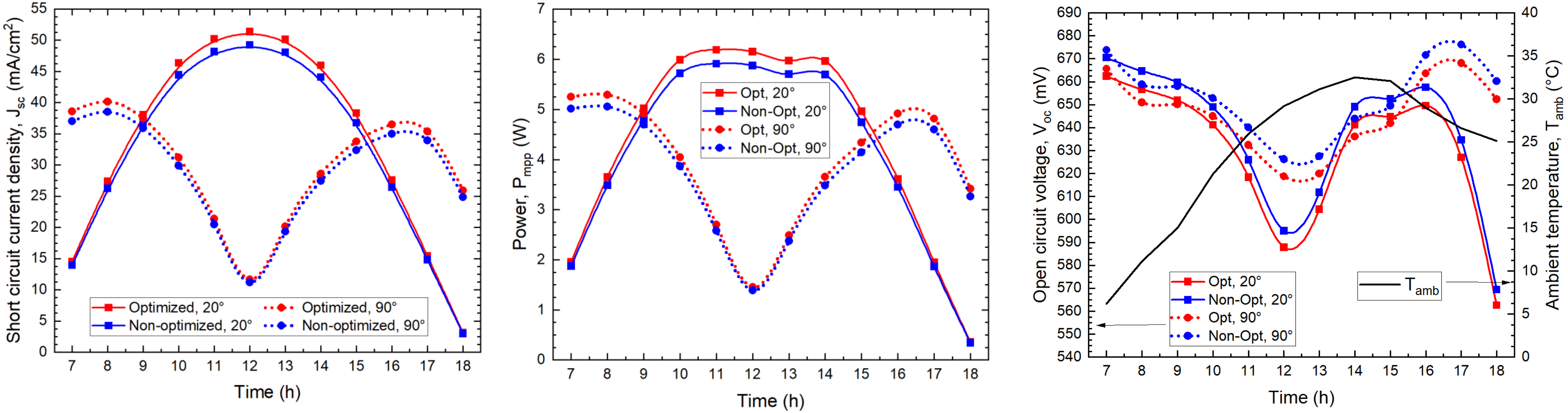

Conclusions and outlook

- The solar cell model is valid for a family of cases
  - Cell structure: p^+nn^+
  - Monofacial and bifacial case
  - For any illumination; only front, only rear or simultaneous
- The model combined with MATLAB allowed to optimize the device under a representative Atacama Spectrum
  - Thickness and doping level of the emitter, cell (base), back surface field
- The model combined with Java allowed to predict the performance for a whole day in Atacama Desert
  - Automation of calculations and less time consumption
- Application to PV module response, provided that absorption of c-Si is known

Thanks for your attention

pablo.ferrada@uantof.cl

MUCOM

UNIVERSIDAD DE MÁLAGA | uma.es

Addlink Software Científico

COMSOL

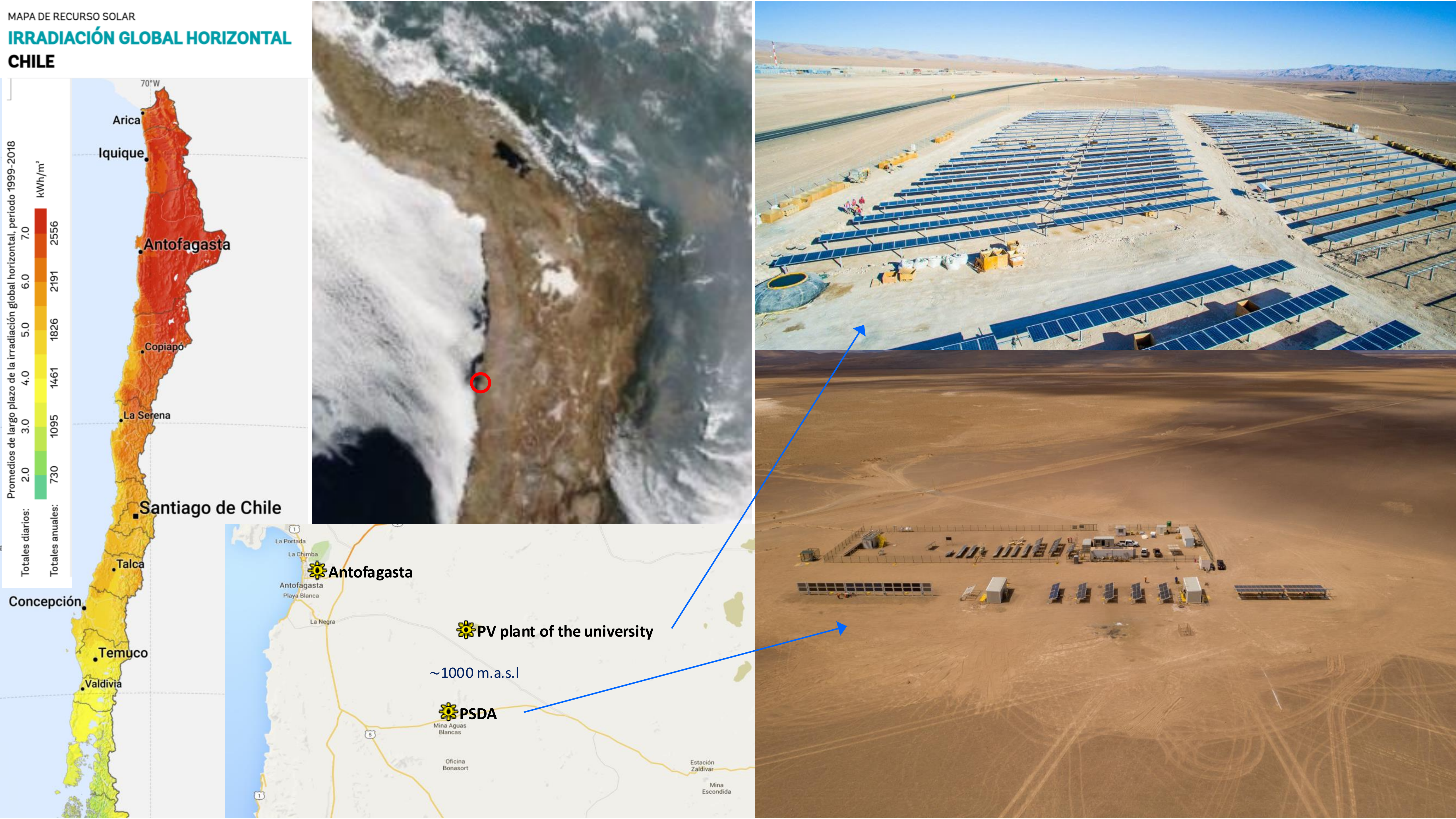
MAPA DE RECURSO SOLAR
IRRADIACIÓN GLOBAL HORIZONTAL
CHILE
70°W
Promedios de largo plazo de la irradiación global horizontal, periodo 1999-2018
kWh/m²
Totales diarios:
Totales anuales:
7.0
6.0
5.0
4.0
3.0
2.0
2556
2191
1826
1461
1095
730
Arica
Iquique
Antofagasta
Copiapó
La Serena
Santiago de Chile
Talca
Concepción
Temuco
Valdivia
La Portada
La Chimba
Antofagasta
Antofagasta
Playa Blanca
La Negra
PV plant of the university
~1000 m.a.s.l
PSDA
Mina Aguas Blancas
Oficina Bonasort
Estación Zaldivar
Mina Escondida

Materials & methods: Data

- Measured and own data
  - Geometrical aspects are known.
  - Doping level was experimentally measured.
  - *Carrier lifetime was* obtained from reference.
  - JV curve under STC (1000 W/m^2, 25°C AM1.5G).

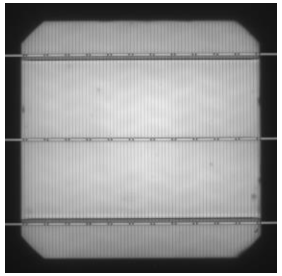

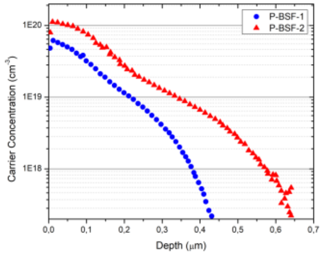

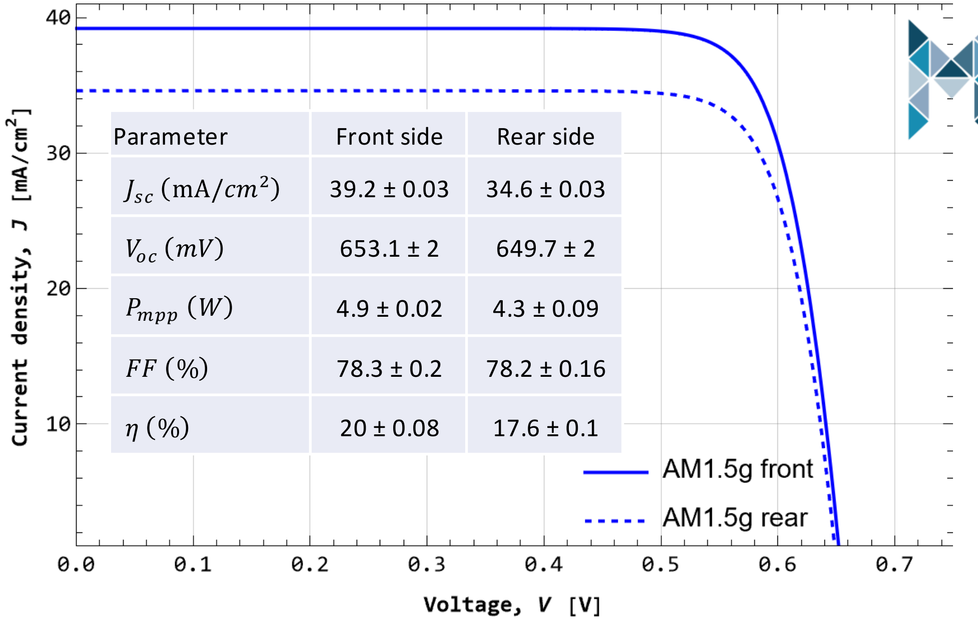

Parameter	Front side	Rear side
J_{sc} (mA/cm^2)	39.2 ± 0.03	34.6 ± 0.03
V_{oc} (mV)	653.1 ± 2	649.7 ± 2
P_{mpp} (W)	4.9 ± 0.02	4.3 ± 0.09
FF (%)	78.3 ± 0.2	78.2 ± 0.16
η (%)	20 ± 0.08	17.6 ± 0.1

P. Ferrada et al. *Interface analysis of Ag/n-type Si contacts in n-type PERT solar cells*. Prog Photovolt Res Appl. 2020;28:358–371.

- Inputs
  - Atmospheric parameters at Platform (PSDA).
  - Atacama Spectra based on **S**imple **M**odel of **A**tmospheric **R**adiative **T**ransfer of **S**unshine.
  - Solar cell temperature
  - Refractive index for c-Si: real and complex.
  - Absorptance of c-Si in a PV module with SunSolve.

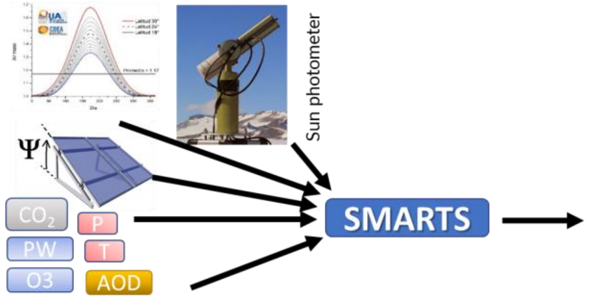

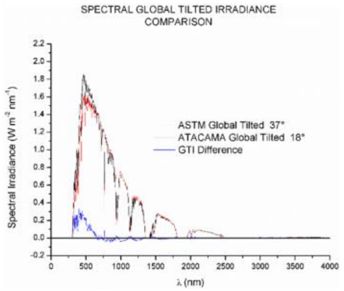

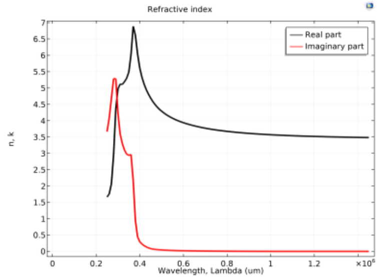

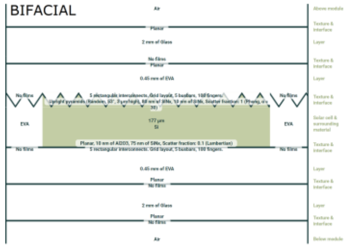

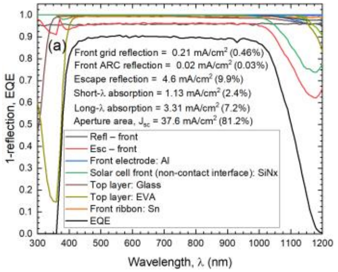

Spectrum of Atacama Desert

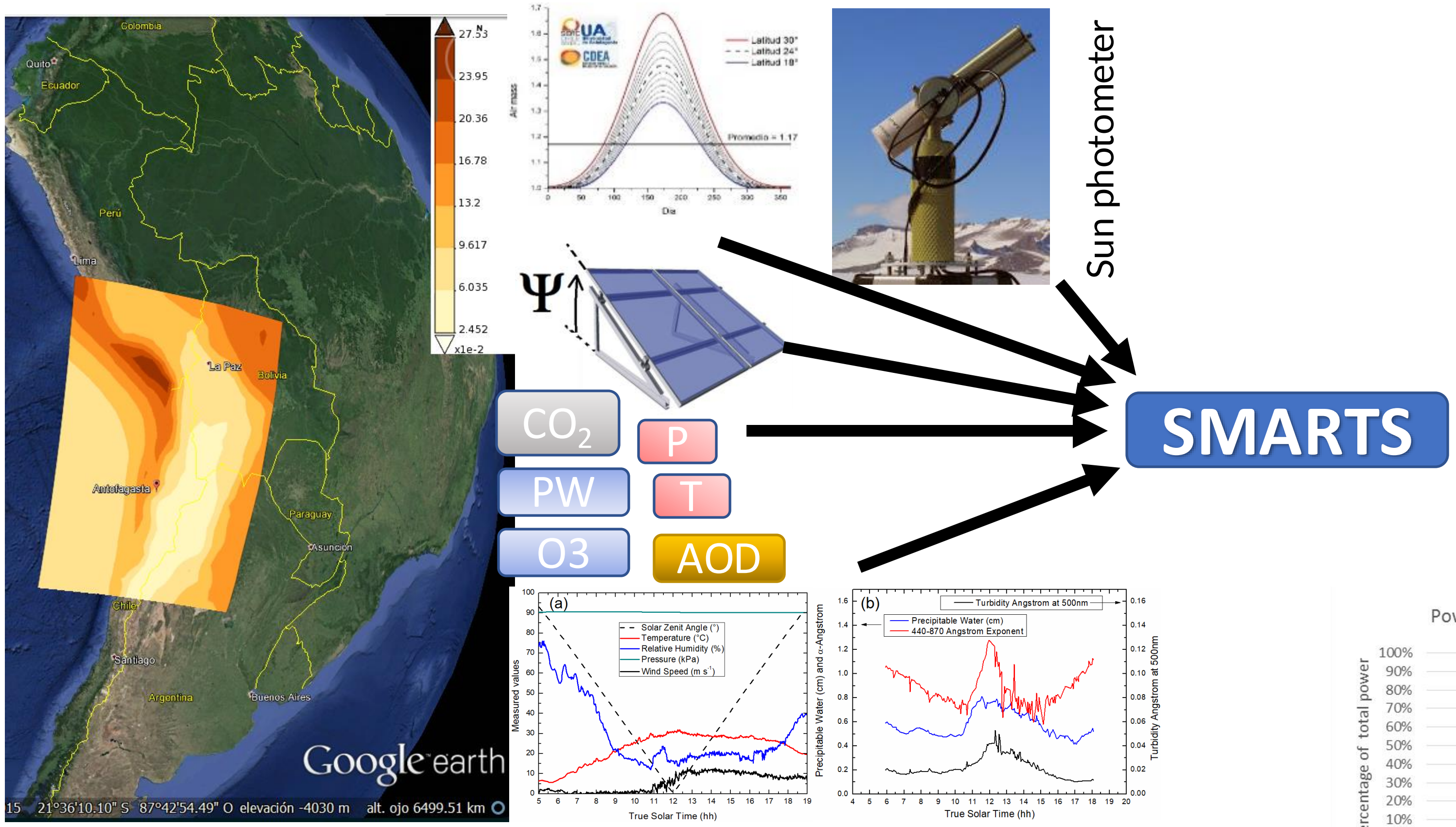

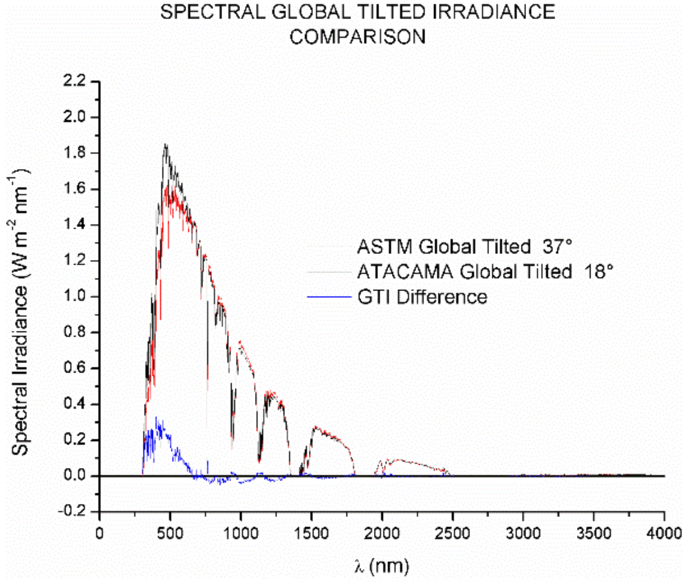

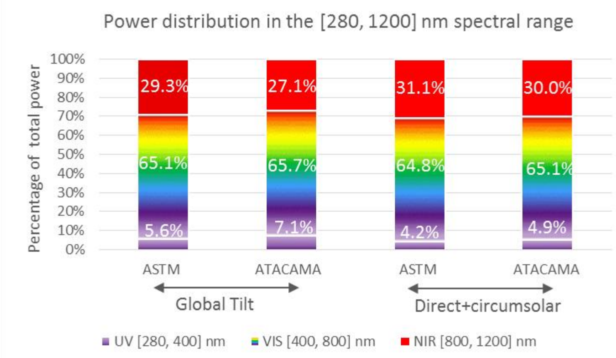

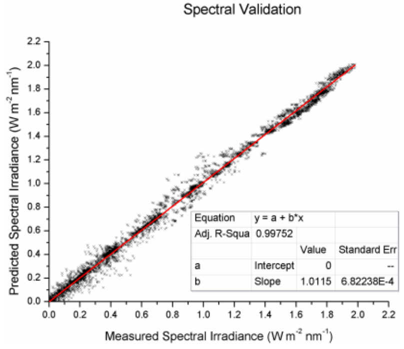

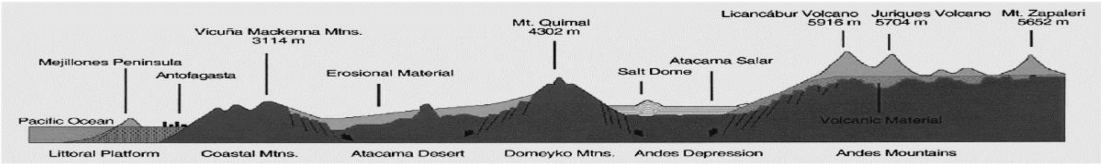

Results & discussion: Mesh independence

- Mesh independence study with voltage from 0 to 1000 mV in steps of 0.1 mV.
- Electrical response (J_{sc}, V_{oc}, P_{mpp} and Eta) vs number of mesh elements.

	Mesh elements	J_{sc} (mA/cm2)	V_{oc} (mV)	P_{mpp} (W)	Eta (%)
Extremely fine	2841	39.296	714.1	5.6064	23.038
Extra fine	1218	39.298	714.1	5.6064	23.038
Finer	643	39.297	714.0	5.6064	23.038
Fine	210	39.277	714.0	5.6029	23.023
Normal	138	39.266	714.0	5.6013	23.016
Coarse	89	39.213	713.9	5.5926	22.981
Coarser	74	39.157	713.9	5.5845	22.947
Extra coarse	62	39.089	713.8	5.5735	22.902
Extremely coarse	47	38.924	713.5	5.58	22.798

$$normalized\ X = X/X_{extremely\ fine}$$

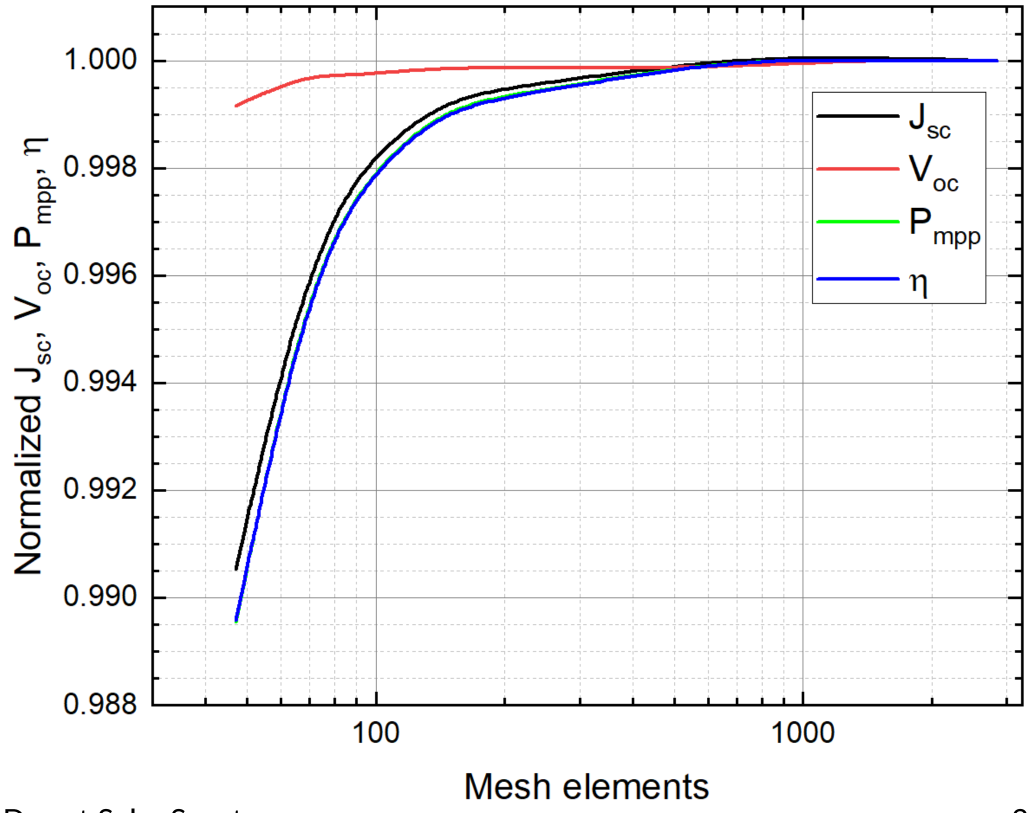

Materials & methods: Optimization

- Optimization in MATLAB
  - Function nPERTopt(x) created from COMSOL model and saved as *m
  - Genetic Algorithm (GA) in MATLAB
  - Script containing input parameters for the GA

- The GA
  - First generation
  - Selection
  - Crossover
  - Mutation
  - Elitism

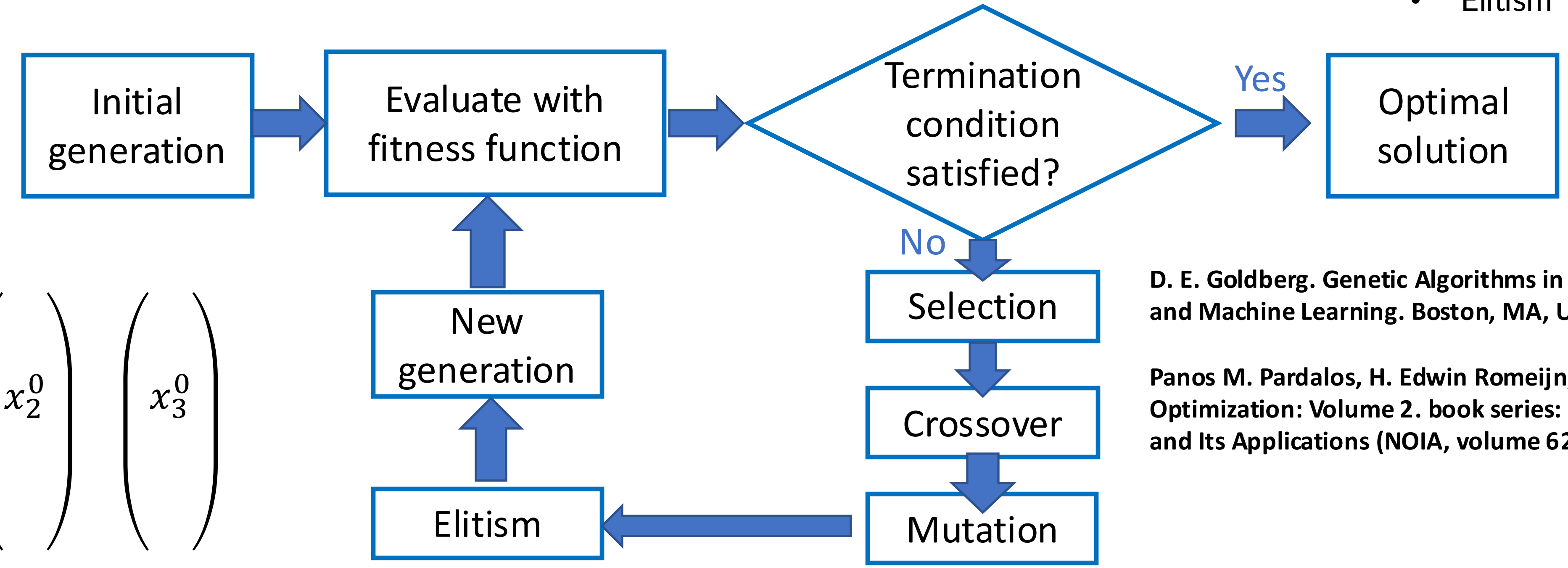

$$\begin{pmatrix} 0.25 \\ 180 \\ 0.5 \\ 2e19 \\ 5e14 \\ 1e20 \end{pmatrix} \quad \begin{pmatrix} x_2^0 \end{pmatrix} \quad \begin{pmatrix} x_3^0 \end{pmatrix}$$

D. E. Goldberg. Genetic Algorithms in Search, Optimization and Machine Learning. Boston, MA, USA, 1989

Panos M. Pardalos, H. Edwin Romeijn, Handbook of Global Optimization: Volume 2. book series: Nonconvex Optimization and Its Applications (NOIA, volume 62). Springer. 2013

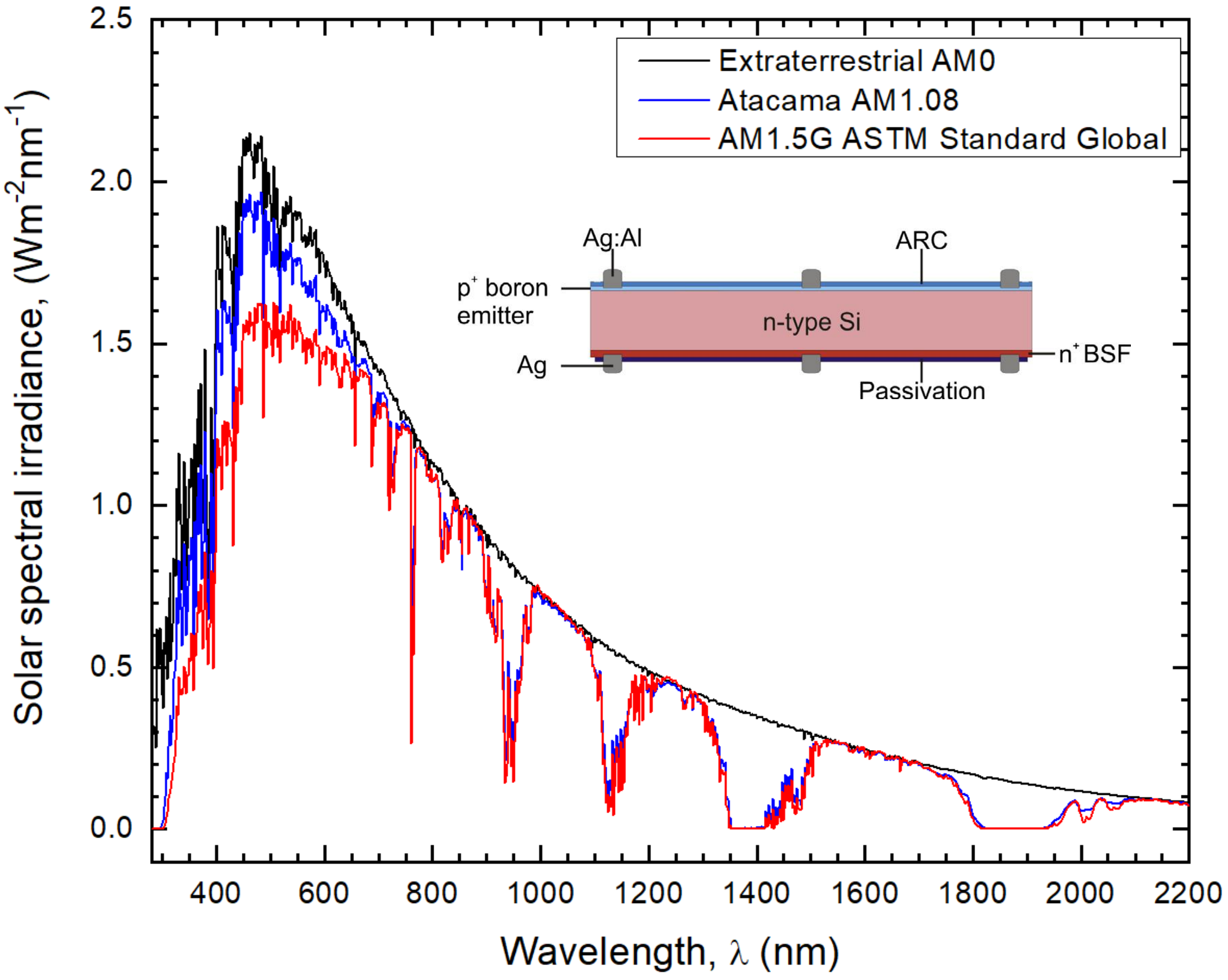

Extraterrestrial AM0
Atacama AM1.08
AM1.5G ASTM Standard Global
Ag:Al
ARC
p+ boron emitter
n-type Si
Ag
n+ BSF
Passivation
Solar spectral irradiance, (Wm-2nm-1)
Wavelength, λ (nm)

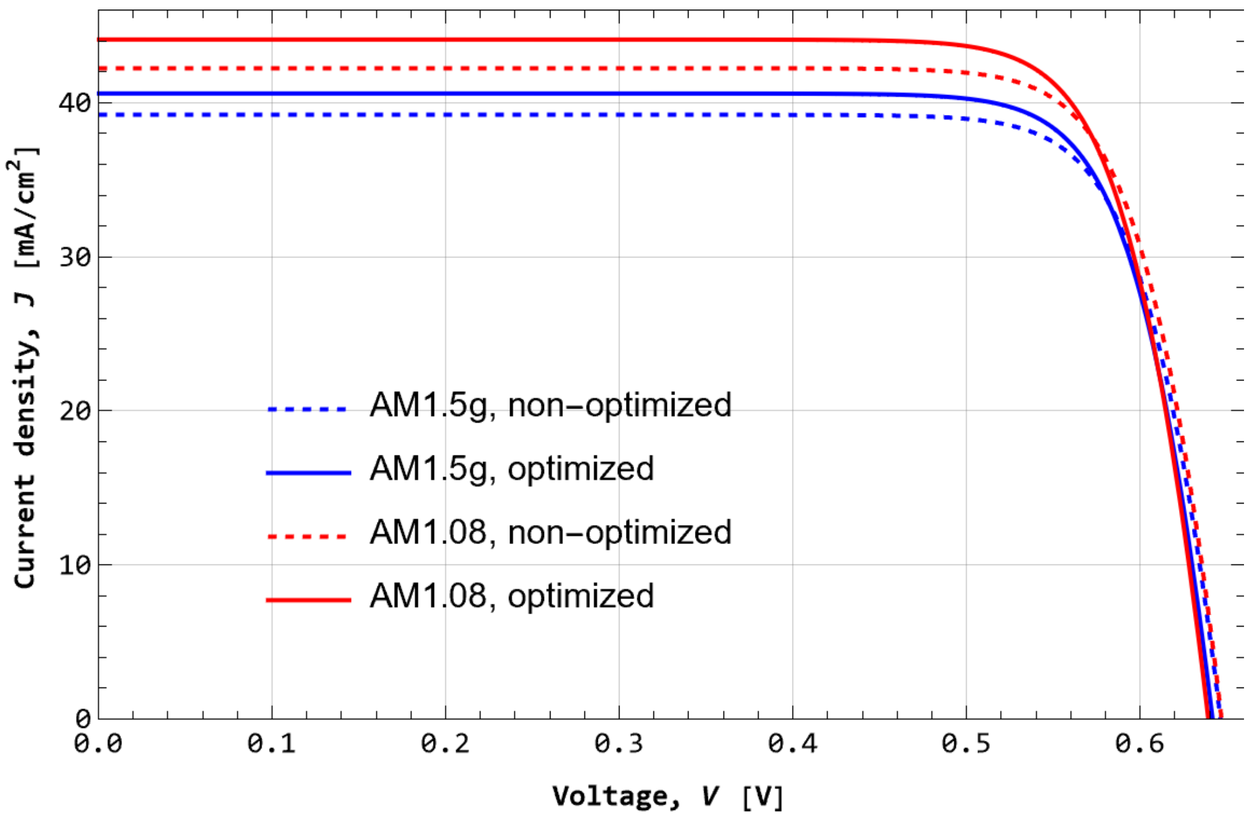

AM1.5g, non–optimized
AM1.5g, optimized
AM1.08, non–optimized
AM1.08, optimized
Current density, J [mA/cm2]
Voltage, V [V]

Atacama Desert Spectra (summer solstice, 2018)

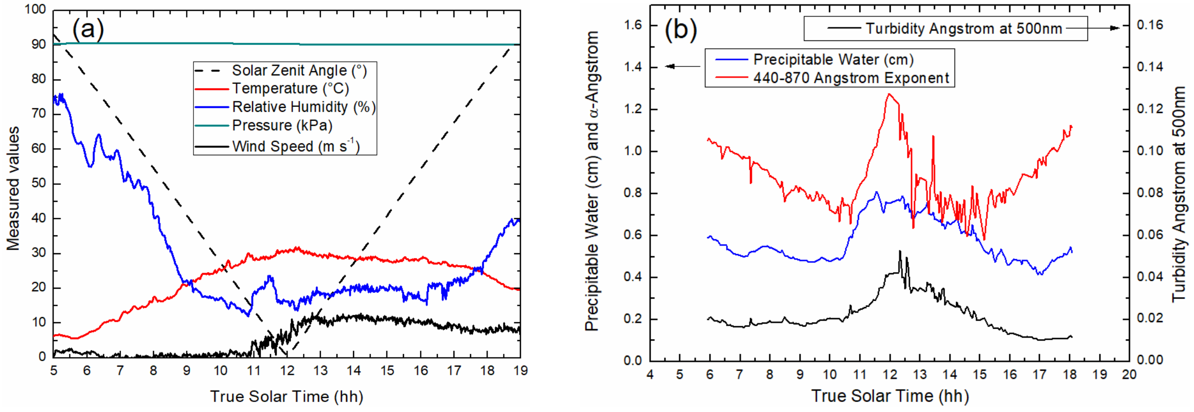

$$\mathrm{AM} \equiv \frac{1}{\sin e + 0.50572\,(6.07995 + e)^{-1.6364}}\,\frac{P}{P_0}$$

$$\mathrm{GTI}_\lambda = \mathrm{DNI}_\lambda \cos\theta + \mathrm{DHI}_\lambda\, r_d + \rho_\lambda\, \mathrm{GHI}_\lambda\, r_r$$

Gueymard, 2019
Kasten and Young, 1989
Perpiñan Lamigueiro, 2012

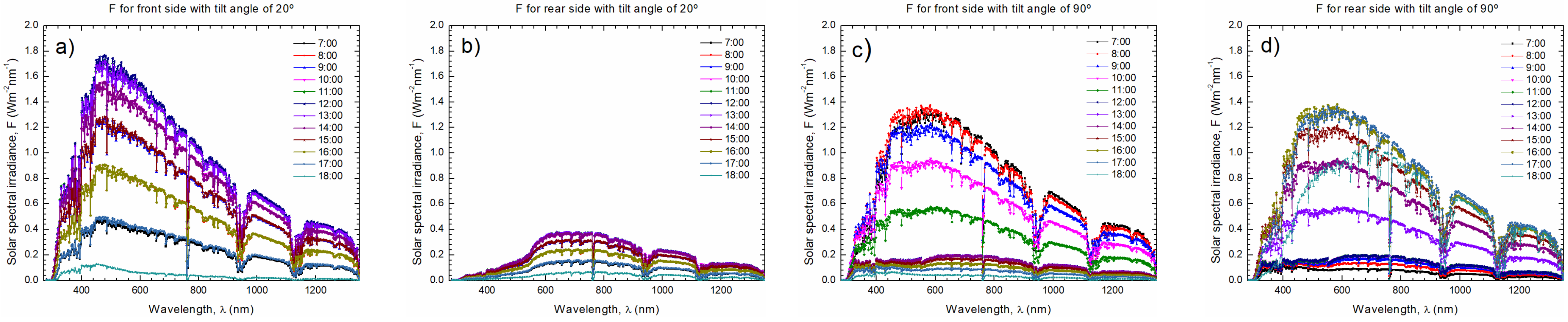

Material degradation

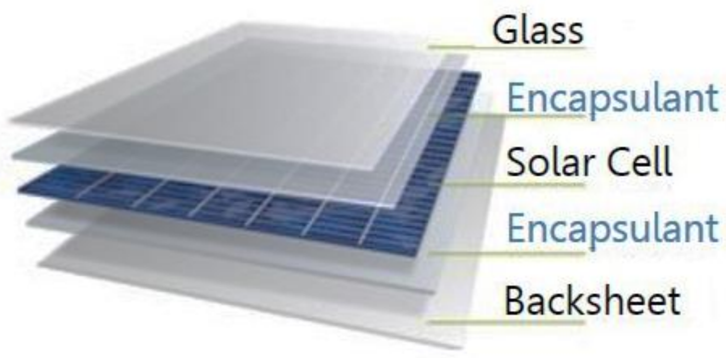

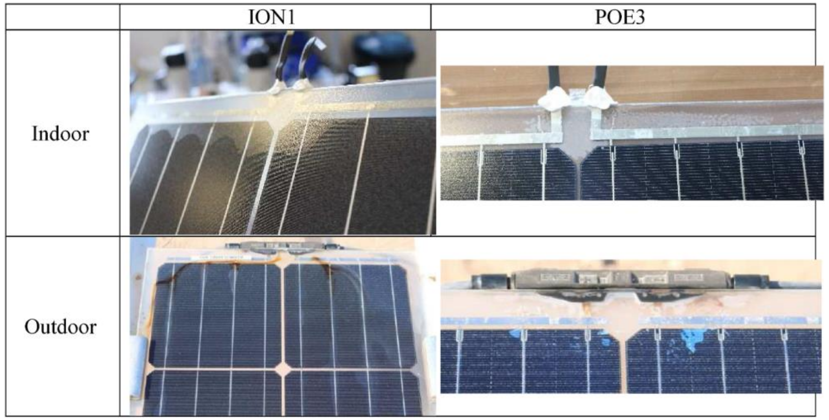

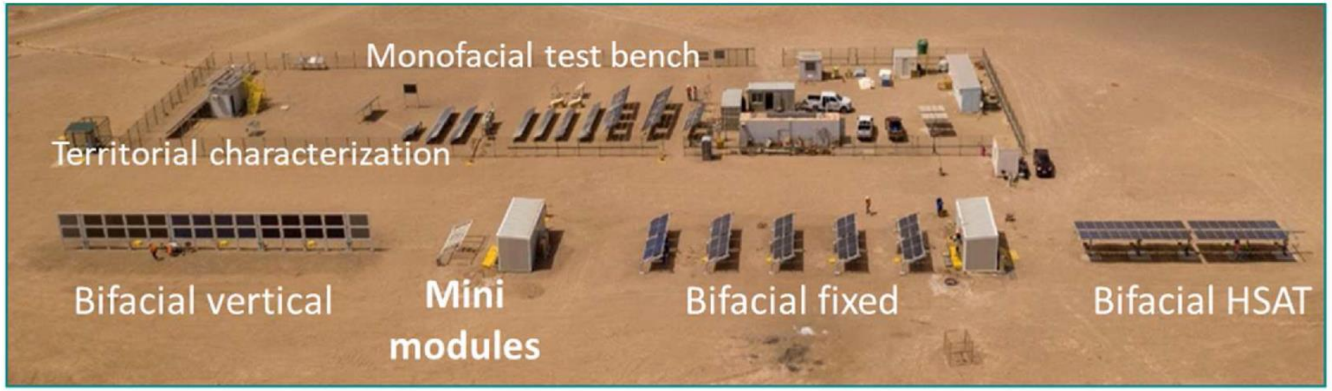

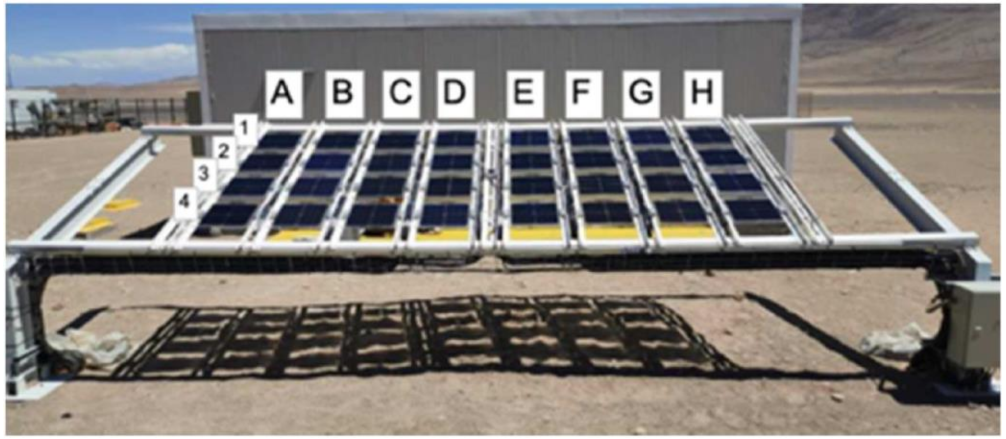

F. Lelievre, R. Couderc, N. Pinochet, L. Sicot, D. Munoz, R. Kopecek, P. Ferrada et al. *Desert label development for improved reliability and durability of photovoltaic modules in harsh desert conditions*. Solar Energy Materials & Solar Cells 236 (2022) 111508.

Theory: mobility

Electron, hole mobility

$$\mu_n = \mu_{min,n} + \frac{\mu_{0,n}}{1+\left(\frac{N}{N_{0,n}}\right)^{\alpha}} \qquad \mu_p = \mu_{min,p} + \frac{\mu_{0,p}}{1+\left(\frac{N}{N_{0,p}}\right)^{\alpha}}$$

Minimum values

$$\mu_{min,n} = \mu_{min,n}^{ref}\left(\frac{T}{T_{ref}}\right)^{\beta_1} \qquad \mu_{min,p} = \mu_{min,p}^{ref}\left(\frac{T}{T_{ref}}\right)^{\beta_1}$$

Reference values

$$\mu_{0,n} = \mu_{0,n}^{ref}\left(\frac{T}{T_{ref}}\right)^{\beta_2} \qquad \mu_{0,p} = \mu_{0,p}^{ref}\left(\frac{T}{T_{ref}}\right)^{\beta_2}$$

Concentration

$$N_{0,n} = N_{0,n}^{ref}\left(\frac{T}{T_{ref}}\right)^{\beta_3} \qquad N_{0,p} = N_{0,p}^{ref}\left(\frac{T}{T_{ref}}\right)^{\beta_3} \qquad N = N_a^- + N_d^+$$

Parameter

$$\alpha = \alpha_{0,n}^{ref}\left(\frac{T}{T_{ref}}\right)^{\beta_4}$$

Loss processes

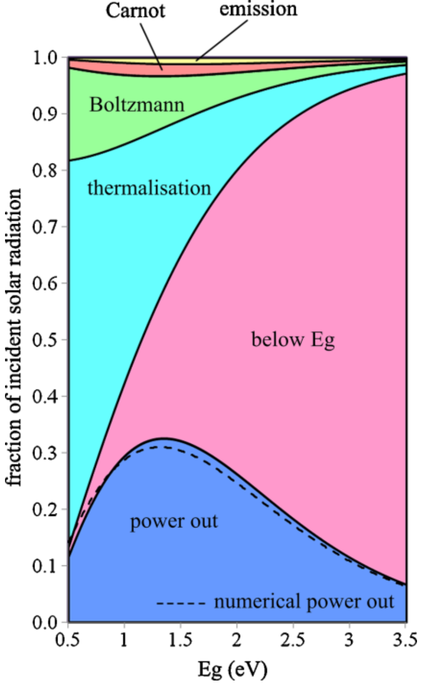

L. C. Hirst, N. J. Ekins-Daukes. *Fundamental losses in solar cells*. Prog. Photovolt: Res. Appl. 2011; 19:286–293.

Intrinsic losses

Boltzmann (angle mismatch): $T_A k_B Ln\left(\frac{\Omega_{Emitt}}{\Omega_{Abs}}\right) = T\Delta S$ → *V*

Carnot (conversion of thermal energy into entropy: $\left(1 - \frac{T_A}{T_S}\right)$ → *V*

Thermalization due to broad spectrum mismatch: $(E_{ph} > E_g)$ → *V*

Transmission due to broad spectrum mismatch: $(E_{ph} < E_g)$ → *J*

Emission to the surroundings (T > 0 K) → *J*

Extrinsic losses

Recombination via traps → *V*

Shunt resistance → V

Series resistance → *J*

Contact shadowing → *J*

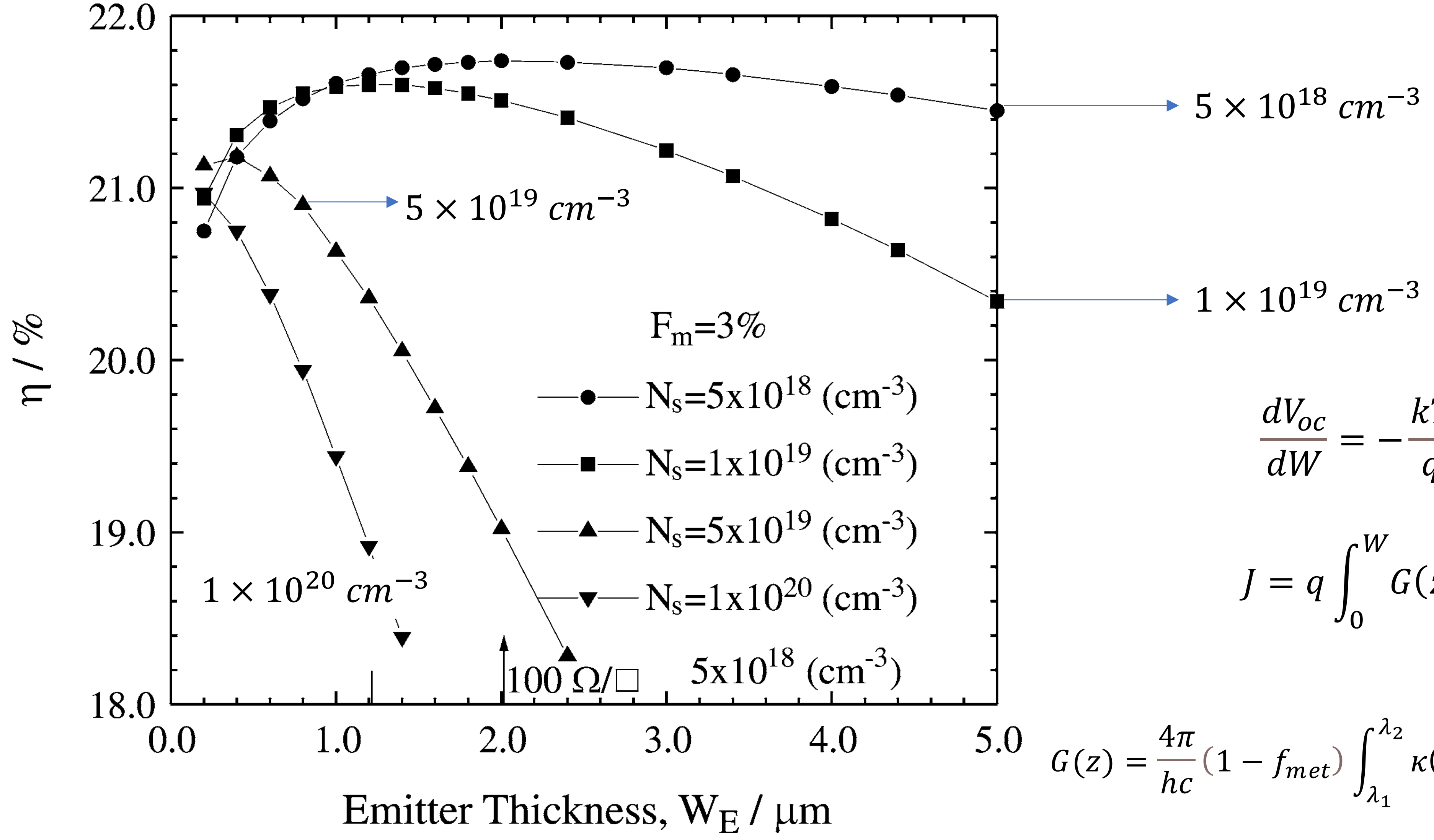

$$\frac{dV_{oc}}{dW} = -\frac{kT}{q}\frac{1}{W}$$

$$J = q\int_0^W G(z)\mathrm{dz}$$

$$G(z) = \frac{4\pi}{hc}(1 - f_{met})\int_{\lambda_1}^{\lambda_2} \kappa(\lambda)\ F(\lambda)\ e^{-\frac{4\pi\ \kappa\ z}{\lambda}}[1 - R(\lambda)]d\lambda$$

N. Stem, M. Cid. Studies of phosphorus Gaussian profile emitter silicon solar cells. Materials Research, Vol. 4, No. 2, 143-148, 2001.

$$\frac{dV_{oc}}{dW} = -\frac{kT}{q}\frac{1}{W}$$

$$J = q\int_0^W G(z)\mathrm{d}z$$

$$G(z) = \frac{4\pi}{hc}(1 - f_{met})\int_{\lambda_1}^{\lambda_2} \kappa(\lambda)\, F(\lambda)\, e^{-\frac{4\pi\,\kappa\, z}{\lambda}}[1 - R(\lambda)]d\lambda$$

Decreasing W → increasing Voltage and decreasing Current Density

Power (*P*) depends on *J V*

The increase in V_{oc} causes *P* to increase more than it decreases due to the reduction of J_{sc}

R. Brendel, H.J. Queisser, On the thickness dependence of open circuit voltages of p-n junction solar cells, Sol. Energy Mater. Sol. Cells. 29 (1993) 397–401.